UPTEC X 01 010
FEB 2001

ISSN 1401-2138

ERIKA SPENS

In vitro profiles of human, rat and mouse fractalkine for rat and mouse chemokine receptor CX_3CR1

Master's degree project

Molecular Biotechnology Programme
Uppsala University School of Engineering

UPTEC X 01 010 | **Date of issue 2001-02**

Author

Erika Spens

Title (English)

In vitro profiles of human, rat and mouse fractalkine for rat and mouse chemokine receptor CX_3CR1

Title (Swedish)

Abstract

In the present study the binding affinities and the intrinsic activities of human, rat and mouse fractalkine (FKN) were investigated at the rat and mouse FKN receptor CX_3CR1, both expressed in HEK-293 cells. The chemokine FKN possesses unique properties among other chemokines by its cystein motif (CX_3C) and by being membrane bound. The extracellular part (FKN(l)) is comprised of a chemokine domain (FKN(s)) carried on top of a mucin-like stalk and it can be proteolytically cleaved to generate soluble FKN. The profiles of both FKN(l) and FKN(s) were investigated and the rank order of potency was determined to be human > rat > mouse at both receptor types. Human and rat FKN(s) exhibited higher affinity than the corresponding FKN(l) while the opposite was true for mouse FKN.

Keywords

fractalkine, neurotactin, chemokine, CX_3C, fractalkine receptor, CX_3CR1, multiple sclerosis

Supervisors

Åsa Malmberg and Maria Wanderoy
AstraZeneca R&D Södertälje, Sweden

Examiner

Åsa Malmberg
AstraZeneca R&D Södertälje, Sweden

Project name	Sponsors
Language **English**	Security
ISSN 1401-2138	Classification
Supplementary bibliographical information	Pages **35**

Biology Education Centre Biomedical Center Husargatan 3 Uppsala
Box 592 S-75124 Uppsala Tel +46 (0)18 4710000 Fax +46 (0)18 555217

In vitro profiles of human, rat and mouse fractalkine for rat and mouse chemokine receptor CX_3CR1

Erika Spens

Sammanfattning

Kommunikation mellan celler i immunförsvaret sker med hjälp proteiner vilka kallas cytokiner. Kemokiner är en grupp inflammatoriska cytokiner som fått mycket uppmärksamhet p.g.a. deras roll vid utvecklandet av neuroinflammatoriska sjukdomar som t.ex. multipel skleros. En kemokin av stort intresse är fraktalkin vilken är unik bland andra kemokiner i att den är bunden till cellmembranet. Den del av proteinet som sitter utanför cellmembranet kan klyvas av och bilda fritt fraktalkin. På så sätt tror man att fraktalkin kan fungera både som signalsubstans för mobilisering av t.ex. vita blodkroppar och som adhesionsmolekyl för de mobiliserade cellerna.

I det här examensarbetet bestämdes och jämfördes affiniteten hos human-, rått- och musfraktalkin. Bindning till rått- och musfraktalkinreceptorn uttryckta i cellinjer studerades. Potensordningen visade sig vara human > råtta > mus. Dessutom testades hur affiniteten hos endast den yttersta delen av det fria fraktalkinet, den s.k. kemokindomänen skilde sig från affiniteten hos hela det fria proteinet. För human- och råttfraktalkin var affiniteten hos kemokindomänen bättre än för hela proteinet medan motsatsen gällde för musfraktalkin.

Examensarbete 20 p i Molekylär bioteknikprogrammet

Uppsala universitet Februari 2001

Table of contents

1 Introduction

1.1 Multiple Sclerosis

Multiple Sclerosis (MS) is a neurological disorder affecting the central nervous system (CNS). The symptoms are weakness, lack of co-ordination as well as impairment of vision and speech. Clinical progression is usually relapsing-remitting with periods of substantial or complete recovery. With time a gradual progression most often develops. The disease is believed to be autoimmune with autoreactive T-cells participating in destroying the myelin sheath of the nerve fibers of the brain and spinal cord. In addition to inflammatory demyelinating lesions, pathological characteristics as axonal loss and scarring may be important in causing irreversible disability (Noseworthy, 1999).

MS affects 1 in 1000 persons of northern European origin residing in temperate climates. Close relatives have a 10-20 times higher risk for developing the disease and there is a female predominance. Little is known about the cause of MS or the factors that contribute to its course. Evidence indicates that MS is a complex trait caused by interactions of genetic and environmental factors, of which viral infections are believed to be one factor of importance.

For decades, corticosteriods have been used to speed recovery from relapses in the treatment of MS. There is also evidence that β-interferon treatment delay clinical progression (Noseworthy,1999). Several strategies for identification of future, more effective, treatment are of major interest. One is directed against pro- and anti-inflammatory cytokines of which fractalkine (FKN; or neurotactin), a chemokine known to be upregulated in brain inflammation (Pan *et. al.*, 1997), is of great interest.

1.2 The chemokine FKN and its receptor

The term chemokine was originally adopted to describe a family of chemoattractant cytokines that induce chemotaxis, tissue extravasation and functional modulation of a wide variety of leukocytes during inflammation (Figure 1). The chemokines are in general smaller (8-10 kD) than inflammatory cytokines and exhibit a characteristic N-terminal cystein motif.

The number and spacing of the cysteins have been used for the classification into CXC (α), CC (β), C (γ) and CX_3C (δ) (Figure 2). FKN was first described in the literature by Bazan *et. al.* in 1997 and is to date the only known member of the δ-class. It is unique among other chemokines by being membrane bound. Human FKN is predicted to be part of a 373-amino acid protein comprised of chemokine domain (76 amino acids; denoted FKN(s); Figure 4) carried on top of a mucin-like stalk (Fong *et. al.*, 2000), a transmembrane spanning region and a C-terminal intracellular part. The extracellular part (i.e. chemokine domain and mucin-like stalk; denoted FKN(l)) can be proteolytically cleaved to generate soluble FKN. The soluble form is a potent chemoattractant for T-cells and monocytes while the membrane-bound form expressed by activated primary endothelial cells is believed to promote adhesion of leukocytes (Bazan *et. al.*, 1997).

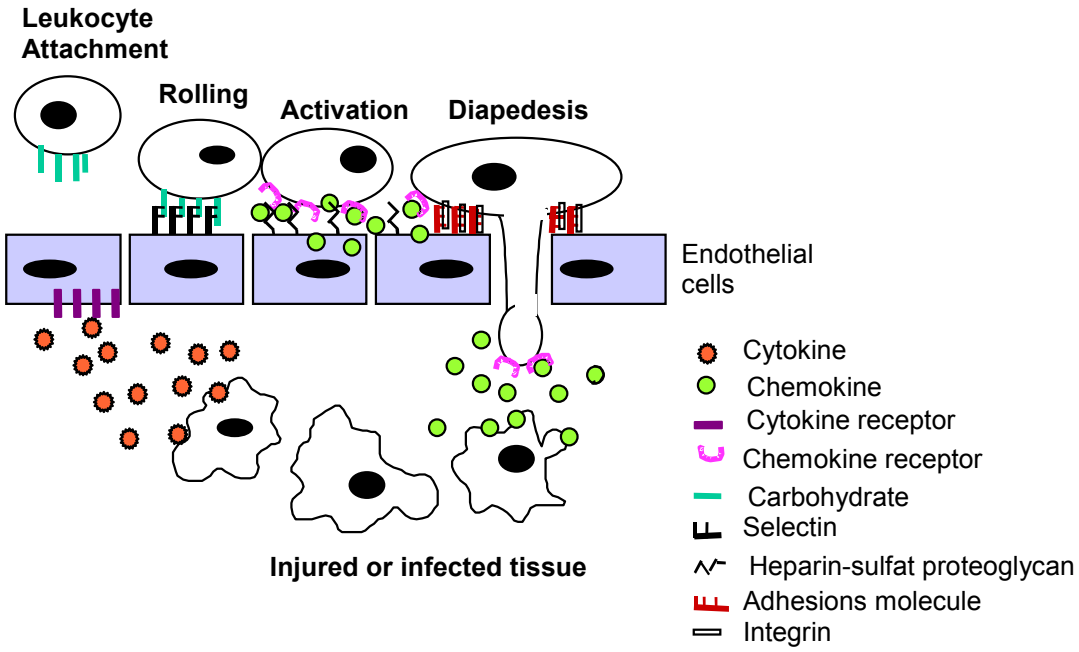

Fig. 1. Inflammation and leukocyte movement. Chemokines are secreted at the site of inflammation by resident endothelial cells and recruited leukocytes, establishing a local concentration gradient. Leukocytes rolling on the endothelium in a selectin mediated manner are retained and chemokine activation of their receptors leads to integrin expression, which in turn leads to capture and extravasation (van Acker *et. al.*, 1996; Luster, 1998).

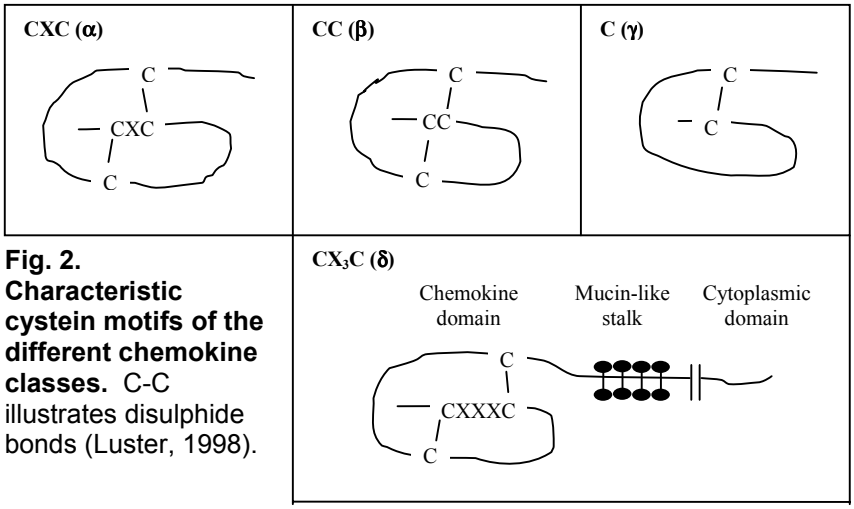

Fig. 2. Characteristic cystein motifs of the different chemokine classes. C-C illustrates disulphide bonds (Luster, 1998).

Chemokines mediate their biological activities via G-protein coupled receptors (GPCR) consisting of seven transmembrane spanning regions. G-proteins are comprised of three subunits (α, β and γ) and are classified into G_s, G_i and G_q-proteins according to the identity of the α-subunit. Each group affects distinct second messenger systems; G_s activates adenylate cyclase (AC) leading to increased synthesis of cAMP, G_i inhibits AC and G_q couples to phospholipase C ultimately leading to intracellular calcium mobilisation. The gene encoding the FKN receptor (CX_3CR1) was first described in the literature by Raport *et. al.* in 1995, termed V28. RNA expression of V28 was found predominantly in neural and lymphoid tissues. A study published in 1997 by Imai *et. al.* suggested that FKN was the endogenous ligand for V28. The receptor was shown to couple to the G_i class of G-proteins since cell migration as well as intracellular calcium mobilisation linked to the CX_3CR1 were found to be *pertussis* toxin-sensitive. Intracellular calcium mobilisation mediated by receptors linked to G_i-proteins is explained by the regulatory function of the $\beta\gamma$-complex on phospholipase C (Morris and Scarlata, 1997; Figure 3).

Intense research efforts focus on the involvement of chemokines in regulating CNS leukocyte migration in immuno-inflammatory disorders. Many cells, intrinsic to the CNS, have the ability to produce chemokines (Asensio and Campbell, 1999). FKN expression is most abundant in the brain but do also occur in kidney, lung and heart. The expression in the CNS is primarily localised to neurones while CX_3CR1 expression is primarily localised to

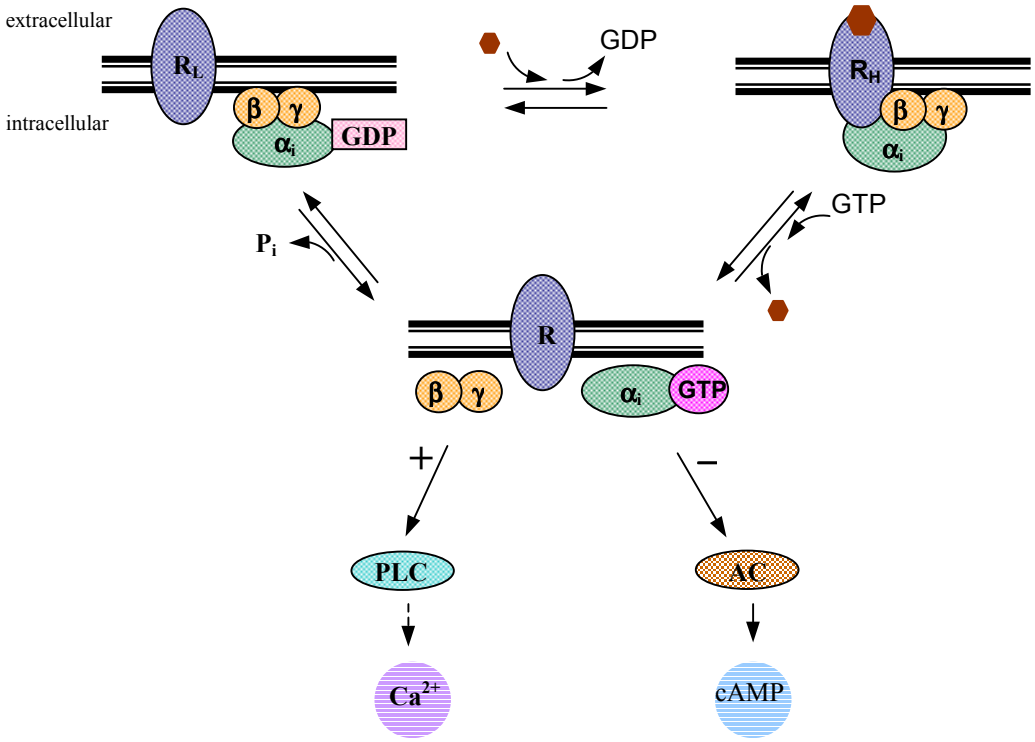

Fig. 3. A possible mechanism for G_i protein mediated signal transduction. Binding of an agonist to the receptor causes guanine exchange (GDP to GTP) at the α-subunit. Upon dissociation from the receptor the α- and βγ-subunits regulate the activity of downstream effectors. The α-subunit inhibit adenylat cyclase (AC) activity leading to decreased levels of cyclic AMP, while the βγ-complex is believed to activates phospholipase C (PLC) ultimately increasing intracellular Ca^{2+} levels (Morris and Scarlata, 1997). Both GDP and GTP reduce the affinity of agonist binding to the receptor. High affinity conformations of the receptor (R_H) are associated with coupling to a nucleotide free G-protein while low affinity conformations (R_L) are associated with an uncoupled receptor (Kent et. al, 1980).

microglia (Harrison et. al. 1998). Putative communication between neurons and microglia mediated by FKN implicates understanding of the normal development of the adult brain (Asensio and Campbell, 1999) as well as understanding of the neurophysiology during pathological states of the CNS. Further evidence for the involvement of FKN in neuroinflammation were presented by Pan *et. al.* in 1997 when induced FKN expression was observed in lipopolysaccaride treated mice. Elevated levels of FKN were also demonstrated in mice with severe experimental autoimmune encephalomyelitis (EAE). Membrane-anchored FKN present on cultured

neurons has been shown to undergo rapid proteolytic cleavage in response to excitotoxic stimulus (Chapman *et. al.*, 2000). This dynamic cleavage followed by chemoattraction of reactive T-cells may represent an early event in the generation and progression of neuro-inflammatory disorders such as MS.

The amino acid (aa) sequence homology of human FKN(s) is; human and rat 83%, human and mouse 78%, and rat and mouse 86%. The extracellular domain of human FKN consists of 318 aa, rat FKN of 310 aa and mouse FKN of 313 aa. The chemokine domain of both human and rat consists of 76 aa while the mouse form is comprised of 81 aa (Pan *et. al.*, 1997). The deduced aa homology of CX_3CR1 is: human and rat 82%, human and mouse 83% and rat and mouse 94%.

1.3 Aim of study

The major objective of this project was to determine the affinity and function of human, rat and mouse FKN at the rat and mouse CX_3CR1 expressed in HEK-293 cells. The potency of both FKN(l) and FKN(s) were tested.

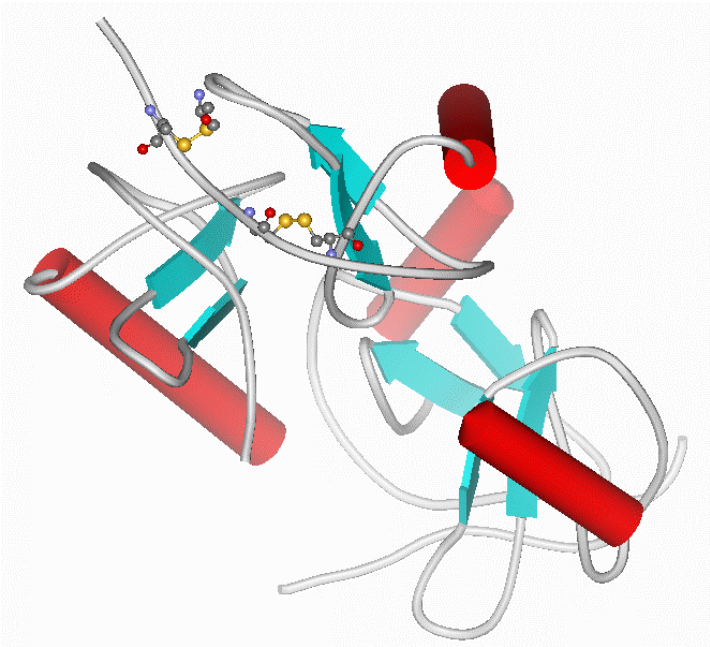

Fig. 4. Structure of human FKN chemokine domain. The four cystein residues constituting the disulphide bonds characteristic for the CX_3C are shown as "ball and stick" (http://www.ncbi.nlm.nih.gov, 14 Feb. 2001).

1.4 Theory of methods

1.4.1 Saturation binding experiments

Saturation binding experiments are performed to obtain receptor density (B_{max}) and the equilibrium dissociation constant (K_D) for a particular radioligand. Total binding is studied through addition of increasing concentrations of radioligand to a fixed concentration of protein. For good reliability the number of concentrations above and below K_D should be equal. Non-specific binding i.e. binding to sites other than the receptor of interest, is determined in the presence of excess unlabeled ligand (>100-fold the K_D). Subtraction of non-specific binding from total binding gives the specific binding of the radioligand to the receptor. Separation of bound radioligand from free radioligand is generally done by rapid filtration through glass fibre filters.

The experimental data is analysed by non-linear regression where B_{max} corresponds to the plateau of the curve for specific binding and K_D the concentration where 50% of the receptors are bound (Figure 5A). In addition, data can be linearized by Scatchard transformation where B_{max} corresponds to the x-axis intercept and K_D the reciprocal slope of the line (Figure 5B).

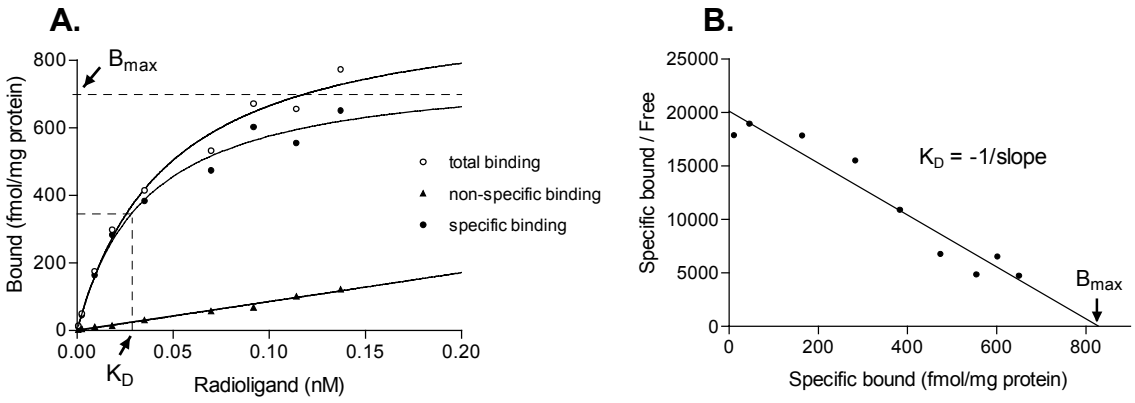

Fig. 5. A typical saturation binding experiment analysed by non-linear regression (A) and Scatchard transformation (B).

Equilibrium receptor binding experiments should be performed without ligand depletion, i.e. the amount of bound ligand should be neglectible. To avoid ligand depletion a simple rule is to keep receptor levels low (0.1x K_D). At K_D, this result in a fraction of bound radioligand that corresponds to less than 10% of added radioligand.

1.4.2 Competition binding experiments

Competition binding experiments are performed to determine the inhibitory constant (K_i) of an unlabeled ligand. Binding of increasing concentrations of unlabeled ligand is studied in the presence of a fixed concentration of a radioligand with known binding profile. The competitive ability of the unlabeled ligand is reflected by the binding of the labeled ligand, yielding a sigmoidal competition curve from which the inhibitory concentration (IC_{50}) is determined (Figure 6). The IC_{50} value is the concentration where the unlabeled ligand inhibits 50% of the maximal specific radioligand binding (E_{max}).

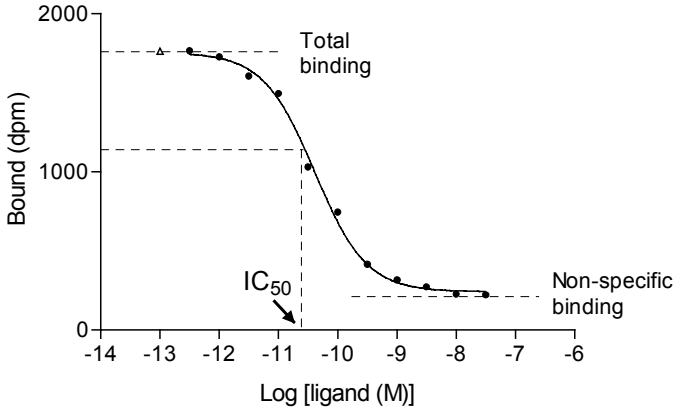

Fig. 6. A typical competition binding curve analysed by non-linear regression.

The K_i value for the unlabeled ligand is calculated by the equation; $K_i = IC_{50}/(1+[L]/K_D)$ where [L] is the concentration of radioligand and K_D its equilibrium dissociation constant (Cheng and Prusoff, 1973).

1.4.3 Scintillation Proximity Assay

The time consuming step of separating bound from free radioligand in filtration binding assays can be avoided by the use of Scintillation Proximity Assay (SPA ; Bosworth and Towers, 1989; Udenfriend *et. al.*, 1987). The method

relies on the use of coated polymer beads containing fluorophors. The SPA beads are directly added to the reaction mixture. Radioisotopes emitting low-energy radiation are required, which effectively transmit their energy to the fluorophors. The Auger electrons of ^{125}I are ideal since they have an average energy of 35 keV and are absorbed in aqueous solution within 35 μm. Beads coated with weatgerm agglutinin (WGA) are preferred at receptor binding studies where carbohydrate residues present on cell membranes bind to the WGA. Binding of radioligand to the immobilised receptor bearing membranes brings the radioisotope in close proximity to the scintillant inside the beads. Emitted photons are amplified and monitored in a scintillation counter. A schematic illustration of SPA is shown in Figure 7.

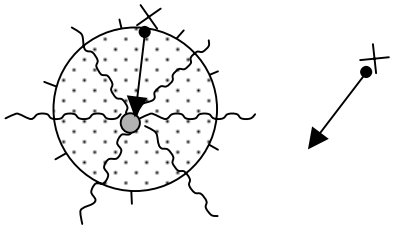

Fig. 7. Schematic illustration of the SPA method. The circle represents a polymer bead coated with WGA and the dot a fluorophor in solid solution. Receptor bearing membranes are immobilised at the surface of the bead by binding to the WGA. The arrow represents the distance travelled by an electron before annihilation or fluorophor capture. The wavy lines emanating from the bead represent emitted light. X: radioligand.

1.4.4 [^{35}S]GTPγS binding experiments

Activation of G-proteins mediated by GPCR is the first step in the signal transduction cascade. Receptors bound with agonist initiate activation of G-proteins by catalysing the exchange of guanosine 5'-diphosphate (GDP) by guanosine 5'-triphosphate (GTP) bound to the α subunit. Upon binding of GTP to the α-subunit the G-protein dissociates from the receptor and regulate the activity of downstream effectors. Hydrolysis of GTP to GDP by the GTPase activity of the α-subunit completes the cyclic process (Figure 3).

The first step of G-protein activation can be studied by binding of radiolabeled non-hydrolysable GTP analogues of which guanosine 5'-O-(γ-[^{35}S]thio)triphosphate ([^{35}S]GTPγS) is the most frequently used (Wieland and Jacobs, 1994). Agonist stimulation of receptor mediated [^{35}S]GTPγS-binding

results in a sigmoidal curve from which the effective concentration (EC_{50}) is calculated (Figure 8). The EC_{50} corresponds to the concentration where the stimulation is 50% of maximal stimulation (E_{max}). In order to suppress basal binding of [^{35}S]GTPγS GDP has to be present. Optimal stimulation also relies on presence of NaCl and Mg^{2+} (Lorenzen *et. al.*, 1993).

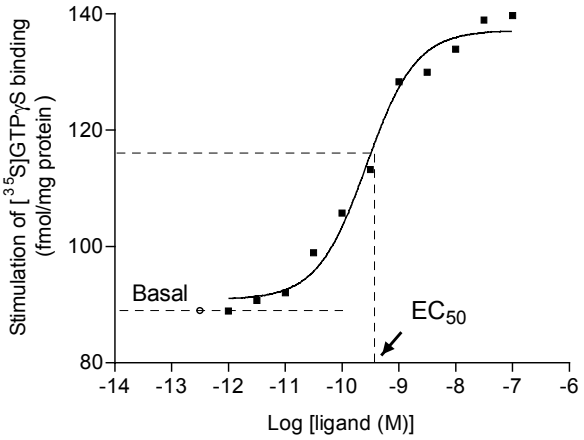

Fig. 8. Receptor mediated stimulation of [^{35}S]GTPγS-binding.

1.4.5 Intracellular calcium measurements

Functional coupling of receptors followed by activation of second messenger pathways involving intracellular calcium release can be studied by the use of fluorescent indicators. Several fluorescent indicators for calcium are available on the market (Grynkiewics *et. al.*, 1985) of which Fura-2 is commonly used because of its unique properties. Fura-2 is introduced into the cell in the form of an ester (fura-2-acetoxymethylester) that passively diffuse across the cell membrane. Once inside the cell the ester is hydrolysed by intracellular esterases yielding a cell-impermeable fluorescent calcium indicator.

The cells are alternately illuminated with UV light at 340 nm and 380 nm and the fluorescence is measured at 510 nm. Unbound Fura-2 exhibits maximum excitation at 380 nm, while the calcium bound form has its maximum at 340 nm. The ratio of the fluorescence intensities (F340/F380) therefore gives a relative measure of intracellular calcium levels (Figure 9).

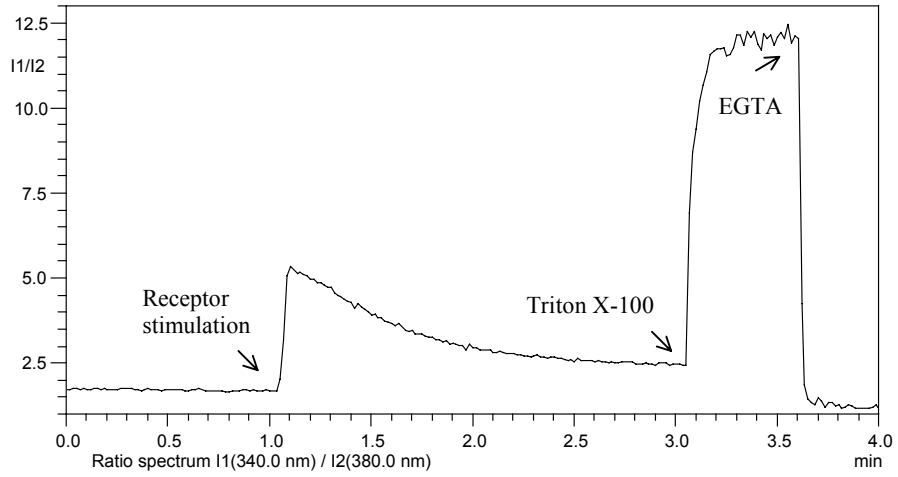

Fig. 9. Fluorescence measurements reflecting the intracellular calcium concentration. The signal is reported as changes in the ratio F340/F380. Calculation of absolute calcium concentration can be done by addition of Triton X-100 and EGTA. Triton X-100 disrupts the cell membrane leading to maximal binding of calcium to Fura-2. EGTA binds with high affinity to Fura-2 allowing measurement of minimal binding.

2 Materials and methods

2.1 Materials

Human embryonic kidney (HEK-293) cells (American type culture collection; Rockville, MD, USA) stably transfected with rat or mouse CX_3CR1 (AstraZeneca R&D Södertälje) were used in the study. The vector pcDNA3 was used for transfection of the rCX_3CR1 and the vector pGEN IRES-neo for the transfection of mCX_3CR1. Both vectors contain a neomycin resistance gene. Cell culture reagents were obtained form Life Technologies (Stockholm, Sweden). Human [^{125}I]FKN(s) (specific activity 2200 Ci/mmol) and [^{35}S]GTPγS (specific activity 1015-1250 Ci/mmol) were purchased from NEN Life Science Products (Boston, MA, USA) and Amersham Pharmacia Biotech (Uppsala, Sweden). WGA coated SPA beads were obtained from Amersham Pharmacia Biotech. Viral MIP-2 and human FKN(s) were purchased from Pepro Tech EC Ltd (London, UK). Human FKN(l), rat FKN(l), mouse FKN(l), human FKN(s), rat FKN(s), a pre-production sample of mouse FKN(s), rat FKN(79 aa) and mouse FKN(84 aa) were obtained from R&D Systems (Oxon, UK). Antisera directed against the N-terminal domain of rCX_3CR1 was produced by Agrisera (Umeå, Sweden). Guanosine-diphosphate (GDP), Gpp(NH)p (5'-guanylylimidodi-phosphate), carbachol (carbamylcholine chloride), triton X-100, probenicid (ρ-[Dipropylsulfanoyl]-benzoic acid), pluronic acid and bacitracin were purchased from Sigma Chemicals Co. (St. Louis, MO, USA). Adenosine 5'-triphosphate (ATP) was bought from Calbiochem-Novabiochem Corporation (Darmstadt, Germany) and EGTA (ethylene glycol bis(β-aminoethyl ether)-N,N,N',N'-tetraacetic acid) from E Merck (Darmstadt, Germany). Fura-2 was purchased from Molecular Probes (Eugene, Oregon, USA). All other chemicals were of analytical grade.

2.2 Cell culture

Recombinant HEK-293 cells were grown in Dulbeccos's Modified Eagles Medium (DMEM) containing Glutamax™, sodium pyruvate, glucose (4500 mg/l) and pyrodixine. The media was supplemented with 10% foetal bovine serum (FBS; heat inactivated) and PEST (100 U penicillin and 100 μg

streptomycin per ml). The cells were grown in 225 cm^2 flasks with ventilated caps (Costar) in 5% CO_2 at 37°C. Geneticin (G418; 400 μg/ml) was used to select cells expressing the CX_3CR1. To avoid reduced receptor expression, the confluence was not allowed to exceed 80%. The cells were detached with 0.05% trypsin and 0.02 % EDTA (ethylenediamine-tetraacetic acid) in phosphate-buffered saline (PBS).

2.3 Membrane preparation

Cells were rinsed twice with PBS, scraped and pooled in harvesting buffer (10 mM Tris-HCl, 5 mM EDTA, 0.1 mg/ml Bacitracin (pH 7.4)) followed by centrifugation at 300 x g for 10 min (4°C). Collected cells were resuspended in harvesting buffer before homogenisation using a Dounce homogeniser. The homogenate was centrifuged at 48 000 x g for 10 min (4°C). The pellet was suspended in harvesting buffer and aliquots were stored at -70°C. Protein concentration was determined using a method modified from Lowry *et. al.*, (1951) with bovine serum albumine (BSA) as standard (Harrington,1990).

2.4 Saturation binding assay

Cell membranes were homogenised using an Ultra-Turrax homogeniser before dilution in binding buffer (50 mM HEPES, 10 mM $MgCl_2$, 1 mM EDTA, 0.5% BSA (pH 7.4)). In experiments using Gpp(NH)p the membranes were pre-incubated with Gpp(NH)p for 45 min at room temperature. Nine concentrations of human [^{125}I]FKN(s) (0.5-150 pM) were used and non-specific binding was determined in the presence of 100 nM human FKN(s). The binding assay was performed in a total volume of 200 μl with 3 μg of protein per tube. Samples were incubated for 2 hours at 30°C. The incubation was terminated by rapid filtration through polyetylenimine (PEI) treated Whatman GF/B filters using a Brandell cell harvester. The filters were washed in cold buffer (10 mM HEPES, 500 mM NaCl, (pH 7.4)). 4 ml of Ultima Gold scintillation fluid (Packard) was added to each sample and radioactivity was measured using a Packman 2500 TR liquid scintillation analyser.

2.5 Competition binding assay

Competition binding experiments were performed in 96-well plates using SPA technique. Cell membranes were homogenised using an Ultra-Turrax homogeniser before dilution in binding buffer (50 mM HEPES, 10 mM $MgCl_2$, 1 mM EDTA, 1% BSA (pH 7.4)). The concentration of human [^{125}I]FKN(s) was 50 pM. Maximal binding was defined with buffer only and minimal binding (equal to non-specific binding) with 100 nM human FKN(s). Each well contained 0.375 mg SPA beads in a total volume of 200 µl. The receptor concentration was approximately 10 pM. The plates were incubated for 3 hours at 30°C before measuring radioactivity in a Trilux Microbeta 1450 plate reader (Wallac, Finland).

2.6 [^{35}S]GTPγS binding assay

Cell membranes were homogenised using an Ultra-Turrax homogeniser before dilution in GTPγS binding buffer (100 mM NaCl, 50 mM Tris-HCl, 10 mM $MgCl_2$, 0.5% BSA (pH 7.4)). The assay was performed in a total volume of 250 µl with 20 µg of protein per tube. The GDP concentration used for experiments with rCX_3CR1/HEK-293 membranes was 3 µM and mCX_3CR1/HEK-293 membranes 1 µM. In experiments aiming at inhibiting the receptor mediated effect using viral MIP-2 or antisera, the membranes were pre-pre-incubated for 15 min at 30°C prior to addition of FKN. Membranes were pre-incubated with GDP and peptide for 30 min at 30°C before addition of [^{35}S]GTPγS followed by another incubation for 30 min at 30°C. The incubation was terminated by rapid filtration through Whatman GF/B filters, using a Brandell cell harvester. The filters were washed in cold buffer (50 mM Tris-HCl, 10 mM $MgCl_2$, (pH 7.4)). 4 ml of Ultima Gold scintillation fluid (Packard) was added to each sample and radioactivity was measured using a Packman 2500 TR liquid scintillation analyser.

2.7 Intracellular calcium measurements

Collected rCX_3CR1-HEK cells, detached with 0.05% trypsin and 0.02 % EDTA in PBS were suspended in HBSS supplemented with 2 mM $CaCl_2$, 10 mM HEPES, 10 mM glucose, 1% BSA, 2.5 mM probenicid (pH 7.4). The cells

were loaded with Fura-2 (2.5-5 μM) for 30-45 min at 25-30°C while shaking. Pluronic acid (0.02-0.04%) was added to the media in order to improve the loading with Fura-2. Henceforward the cells were kept in the dark. Loading was terminated by centrifugation at 180 x g for 10 min. The cells were washed once in HBSS before recentrifuged at 180 x g for 2 min. Experiments were run in a cuvette with stirring. 1 million cells in a total volume of 350 μl HBSS were used for each study. Fluorescence at 510 nm was measured at excitation wavelengths of 340 nm and 380 nm alternatively, using a fluorescence spectrophotometer (Shimadzu RS-5301PC).

2.8 Data analysis

In the saturation binding experiments some ligand depletion was difficult to avoid. The dpm values of total binding were therefore subtracted from the dpm of added ligand (total counts), to calculate the number of dpm free in solution. All binding data were analysed by non-linear regression analysis using PRISM 3.00 (Graphpad Software, San Diego, CA). One- and two-site curve fitting were tested in the competition experiments. The two-site model was accepted when the curve-fit was significantly improved ($p<0.05$; F-test). The [^{35}S]GTPγS-binding data were analysed by sigmoidal dose-response curve fitting. Statistical comparisons were made with Student's unpaired t-test or with ANOVA followed by Bonferroni's Multiple Comparison Test.

3 Results

3.1 [^{125}I]FKN(s) saturation binding

Saturation binding experiments demonstrated that human [^{125}I]FKN(s) binds with high affinity to the cloned rat and mouse CX_3CR1 expressed in HEK-293 cells (rCX_3CR1: K_D = 23.6 pM and rCX_3CR1: K_D = 30.7 pM) (Table 1). Experiments were also performed in the presence of Gpp(NH)p, a non-hydrolysable GTP-analogue that uncouple the receptor from the G-protein (Milligan and Unson, 1989). A slight, but not significant, decrease was observed in the presence of Gpp(NH)p (Figure 10).

TABLE 1

Saturation binding of human [^{125}I]FKN(s) to the rat and mouse CX_3CR1

Saturation experiments were performed as described in Materials and Methods. Experiments were also performed in the presence (+) of Gpp(NH)p. Results are means ± SEM of n experiments. Corresponding Scatchard analyses were in good agreement with the results obtained by non-linear regression. ND: not determined.

	Rat CX_3CR1		Mouse CX_3CR1	
	K_D	n	K_D	n
	pM		*pM*	
	23.6 ± 7.9	4	30.7 ± 4.4	3
+ Gpp(NH)p	45.3 ± 23.6	2	ND	

The receptor density (B_{max}) of the mCX_3CR1 was 580 ± 30 fmol/mg of protein (n=3). Two membrane preparations of the rCX_3CR1 were made. The first yielded a receptor density of 810 ± 80 fmol/mg of protein (n=2) and the second a density of 240 ± 70 fmol/mg of protein (n=2). The much lower density obtained in the second membrane preparation may be due to the higher confluence of the cells at the time of harvest (100% compared to 80%). Too high confluence of receptor expressing HEK-293 cells has previously been observed to diminish receptor expression.

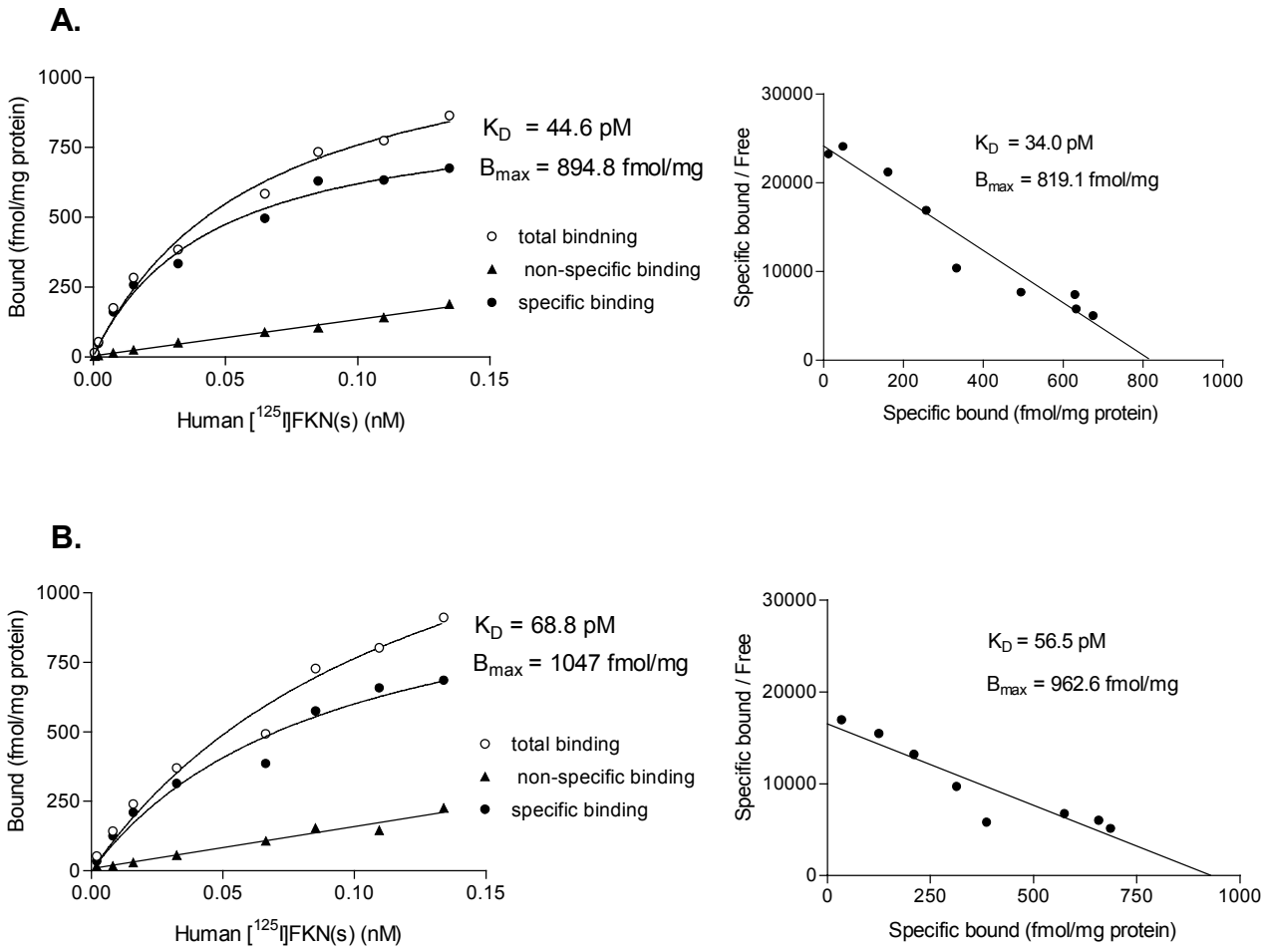

Fig. 10. Representative saturation binding curves for human [^{125}I]FKN(s) to the rCX$_3$CR1 in the absence (A) and the presence (B) of Gpp(NH)p. Corresponding Schatchard plots are shown to the right.

3.2 Human, rat and mouse FKN competition binding

The affinities of human, rat and mouse FKN(l) and FKN(s) were determined for rCX$_3$CR1 and mCX$_3$CR1. Additional forms of rat and mouse FKN(s) comprised of three extra amino acids (aa) N-terminally of the chemokine domain (denoted 3rFKN(s) and 3mFKN(s)) were also tested. The complete aa sequence of the different forms of FKN(s) are shown in Figure 11.

TABLE 2 **Affinities of human, rat and mouse FKN for the rat and mouse CX_3CR1**

The competition experiments with human [^{125}I]FKN(s) were performed using SPA technique as described in Materials and Methods. Results are means ± SEM of n experiments.

Data were analysed with one- and two-site curve fitting. K_h and K_l obtained from the two-site curve fit represent affinity for receptors in the high- and low affinity states. R_h indicates the percentage of receptors in the high affinity state.

Statistical comparisons were made with unpaired t-test or with ANOVA followed by Bonferroni's Multiple Comparison Test.

		Rat CX_3CR1			Mouse CX_3CR1		
Peptide		Affinity	R_h	n	Affinity	R_h	n
		nM	*%*		*nM*	*%*	
hFKN(l)	K_i	0.144 ± 0.033[a,b,c]		3	0.273 ± 0.021[b,d]		5
	K_h	0.072 ± 0.003	63	2[e]	0.060	47	1[e]
	K_l	1.3 ± 0.2		2	1.2		1
rFKN(l)	K_i	0.268 ± 0.069[f]		3	0.960 ± 0.280		5
	K_h	0.076 ± 0.017	55	3[e]	0.091 ± 0.018	42	4[e]
	K_l	4.4 ± 1.0		3	4.6 ± 1.0		4
mFKN(l)	K_i	0.536 ± 0.081[g]		3	2.1 ± 0.7[g]		5
	K_h	0.072 ± 0.027	39	3[e]	0.369 ± 0.272	34	2[e]
	K_l	5.9 ± 3.2		3	20.9 ± 17.0		2
hFKN(s)	K_i	0.018 ± 0.003[h]		3	0.022 ± 0.003[i]		4
rFKN(s)	K_i	0.112 ± 0.013[h]		3	0.298 ± 0.071[i]		6
	K_h	0.013 ± 0.005	38	3[e]	0.056 ± 0.016	49	5[e]
	K_l	0.488 ± 0.116		3	2.7 ± 0.7		5
mFKN(s)	K_i	2.3 ± 0.6		2	9.1 ± 2.7		2
3rFKN(s)	K_i	184 ± 118		2	102 ± 35		2
3mFKN(s)	K_i	19.5 ± 0.5		3	26.3 ± 9.0		6
vMIP-2	K_i	102 ± 3		2	179 ± 5		2

[a] Comparison of K_i for human FKN(l) between receptors (Student's t-test; $p<0.05$).

[b] Comparison of K_i for human FKN short and long at $rCX_3CR1$and mCX_3CR1, respectively (Student's t-test; rCX_3CR1: $p<0.05$; mCX_3CR1: $p<0.001$).

[c] Comparison of K_i for human, rat and mouse FKN(l) at rCX_3CR1 (ANOVA; hFKN(l) versus mFKN(l): $p<0.05$).

[d] Comparison of K_i for human, rat and mouse FKN(l) at mCX_3CR1 (ANOVA; hFKN(l) versus mFKN(l): $p<0.05$).

[e] Number of experiments with significantly better fit with two-site analysis.

[f] Comparison of K_i for rat FKN short and long at mCX_3CR1 (Student's t-test; $p<0.05$).

[g] Comparison of K_i for mouse FKN short and long at rCX_3CR1 and mCX_3CR1 (Student's t-test; rCX_3CR1: $p<0.05$; mCX_3CR1: $p<0.05$).

[h] Comparison of K_i for human, rat and mouse FKN(s) at rCX_3CR1 (ANOVA; hFKN(s) versus mFKN(s): $p<0.01$; rFKN(s) versus mFKN(s): $p<0.01$).

[i] Comparison of K_i for human, rat and mouse FKN(s) at mCX_3CR1 (ANOVA; hFKN(s) versus mFKN(s): $p<0.001$; rFKN(s) versus mFKN(s): $p<0.001$).

h-QHHGVTKCNITCSKMTSKIPVALLIHYQQNQASCGKRAIILETRQHRLFCADPKEQWVKDAMQHLDRQAAALTRNG

r-*LAG*QHLGMTKCNITCHKMTSPIPVTLLIHYQLNQESCGKRAIILETRQHRHFCADPKEKWVQDAMKHLDHQTAALTRNG

m-*LPG*QHLGMTKCEIMCGKMTSRIPVALLIRYQLNQESCGKRAIVLETTQHRRFCADPKEKWVQDAMKHLDHQAAALTKNGGKFEK

Fig. 11. Amino acid sequences of FKN(s) as produced and sequenced by R&D Systems (Oxon, UK). Letters in italics represent the three additional amino acids present in 3rFKN(s) and 3mFKN(s). Cystein residues in blue constitute the characteristic chemokine disulphide bonds. Residues in red in the rat (r) and mouse (m) sequences represent non-conservative amino acid differences compared to the human (h) sequence.

In general, all chemokines tested showed a higher affinity for rCX$_3$CR1 compared to mCX$_3$CR1 (Table 2). The rank order of potency for FKN(I) and FKN(s) were human > rat > mouse. The affinity of rat FKN(I) compared to human FKN(I) was approximately 2- and 3-fold lower at the rCX$_3$CR1 and mCX$_3$CR1, respectively. Corresponding comparison for mouse FKN(I) revealed a 4- and 10-fold difference. Representative competition binding curves for FKN(I) are shown in Figure 12.

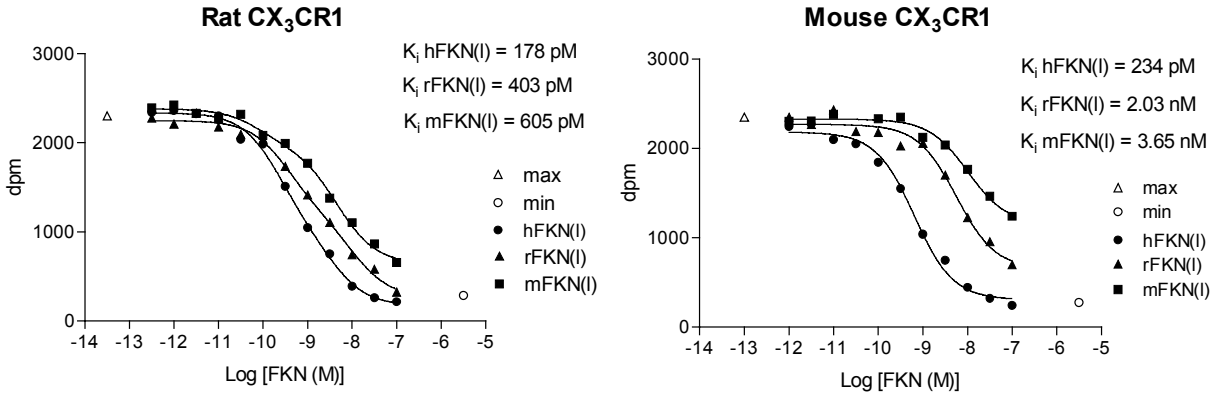

Fig. 12. Representative competition binding curves for human, rat and mouse FKN(I) binding to the rCX$_3$CR1 and mCX$_3$CR1.

The affinity of rat FKN(s) was approximately 10-fold lower than for human FKN(s) at both receptor types. Mouse FKN(s) possessed considerably lower affinity; 100 and 400 times lower than human FKN(s) at the rCX$_3$CR1 and mCX$_3$CR1, respectively. The affinties of 3rFKN(s) and 3mFKN(s) were shown to be very low (Table 2).

The affinities of human and rat FKN(s) compared to the corresponding long were significantly higher for both receptor types with the exception of rat FKN at the rCX$_3$CR1. The approximate affinity difference was for human FKN 10-fold and for rat FKN 3-fold. For mouse FKN the opposite was true; the short form exhibited a significant 4-fold lower affinity as compared to the long at both receptors.

The competition data were analysed with one and two-site curve fitting. In homologous competition experiments (i.e. human [^{125}I]FKN(s) versus human FKN(s)) the binding was mono-phasic. This was also observed for mouse FKN(l) and FKN(s). The other versions of FKN were best described with a two-site model (Table 2).

TABLE 3

Effect of the GTP-analogue Gpp(NH)p on FKN binding

Competition experiments in the absence and presence of Gpp(NH)p were performed as described in Materials and Methods. The used K_D values for human [^{125}I]FKN(s) were 23.6 pM and 30.7 pM for the rat and mouse CX$_3$CR1 as determined in the absence of Gpp(NH)p (Table 1). Results are means ± SEM of 2 experiments.

	Rat CX$_3$CR1	Mouse CX$_3$CR1
Peptide	K_i	K_i
	nM	*nM*
hFKN(s)	0.026 ± 0.000	0.032 ± 0.005
+ Gpp(NH)p	0.024 ± 0.006	0.032 ± 0.004
rFKN(s)	0.693 ± 0.038	2.4 ± 1.1
+ Gpp(NH)p	2.3 ± 0.8	6.4 ± 0.8
mFKN(s)	2.3 ± 0.6[a]	9.1 ± 2.7[a]
+ Gpp(NH)p	7.2 ± 1.7	30.3 ± 13.7

[a] Data from Table 2.

Significantly better fit with the two-site model indicates binding to different receptors or different conformations of the same receptor. In this case the data in assumed to represent binding to high- and low affinity conformation of the CX$_3$CR1 (Figure 3). The GTP-analogue Gpp(NH)p shifts the receptors towards the low affinity state. Experiments performed with FKN(s) in the absence and presence of Gpp(NH)p revealed an approximate 3-fold decrease in affinity for rat and mouse, indicating that the receptor conformation states are slightly dependent on receptor G-protein coupling (Table 3). Human

FKN(s) was, however, unaffected by Gpp(NH)p. There is a discrepancy in affinity for rat FKN(s) presented in Table 2 and 3 which is due to different batches/shipments of the peptide.

The chemokine receptor antagonist vMIP-2 (macrophage inflammatory protein) displayed low affinity (K_i >100 nm) for the rat and mouse CX_3CR1.

3.3 CX_3CR1-mediated [^{35}S]GTPγS-binding

Functional G-protein coupling of the rat and mouse CX_3CR1 were examined using [^{35}S]GTPγS-binding assay. Binding of [^{35}S]GTPγS to G-proteins was stimulated with the various FKN peptides. The results are summarised in Table 4. Representative [^{35}S]GTPγS-binding curves for FKN(I) are shown in Figure 13.

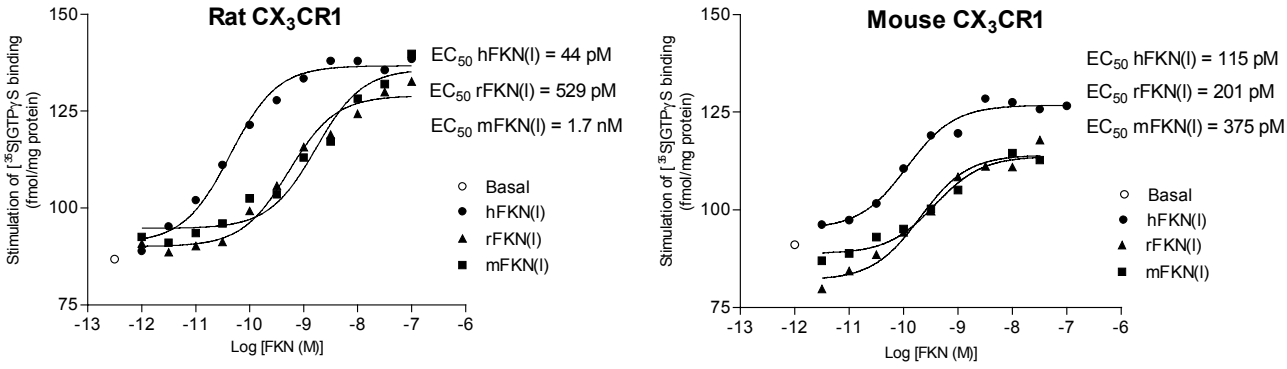

Fig. 13. Representative [^{35}S]GTPγS binding experiments. Stimulation with human, rat and mouse FKN(I) at the rCX_3CR1 and mCX_3CR1 are illustrated.

The efficacy (E_{max}) of mouse FKN(I) differed significantly compared to human and rat FKN(s) at the mCX_3CR1. Otherwise all versions of FKN(I) and FKN(s) tested were able to stimulate [^{35}S]GTPγS binding via the rCX_3CR1 and mCX_3CR1 to the same extent. The rank order of potency for both FKN(I) and FKN(s) were human > rat > mouse as observed in the competition binding experiments. The potencies of mouse FKN(I) and FKN(s) were lower than the potencies of human and rat. Later batches/shipments of mouse FKN(I) displayed considerably lower potency (160 pM (n=1) compared to 1.2 nM

(n=4) at the rCX$_3$CR1 and 317 pM (n=3) compared to 2.2 nM (n=2) at the mCX$_3$CR1) making interpretation of the data difficult. Preliminary experiments showed that the potencies of 3rFKN(s) and 3mFKN(s) where very low at both the rat and mouse CX$_3$CR1.

TABLE 4

Rat and mouse CX$_3$CR1-mediated [^{35}S]GTPγS binding stimulated with human, rat and mouse FKN

[^{35}S]GTPγS-binding experiments were performed as described in Materials and Methods. Results are means ± SEM of n experiments. Statistical comparisons were made with unpaired t-test or with ANOVA followed by Bonferroni's Multiple Comparison Test.

	Rat CX$_3$CR1			Mouse CX$_3$CR1		
Peptide	EC_{50}	E_{max}	n	EC_{50}	E_{max}	n
	nM	*fmol*		*nM*	*fmol*	
hFKN(l)	0.058 ± 0.008[a,b]	37	3	0.154 ± 0.046	37	3
rFKN(l)	0.424 ± 0.131	41	5	0.357 ± 0.092	31	5
mFKN(l)	1.7 ± 0.5	41	5	1.1 ± 0.5	25[c]	5
hFKN(s)	0.019 ± 0.008[d]	44	3	0.049 ± 0.014[e]	41	3
rFKN(s)	0.165 ± 0.055[d]	45	3	0.275 ± 0.045[e]	39	3
mFKN(s)	1.5 ± 0.4	39	3	1.5 ± 0.03[e]	31	3
3rFKN(s)	77.8	14	1	295	11	1
3mFKN(s)	61.6	21	1	137	19	1
vMIP-2	NR[f]			NR[f]		

[a] Comparison of EC_{50} for human FKN short and long at rCX$_3$CR1 (Student's t-test; $p<0.05$).

[b] Comparison of EC_{50} for human, rat and mouse FKN(l) at rCX$_3$CR1 (ANOVA; hFKN(l) versus mFKN(l): $p<0.05$).

[c] Comparison of E_{max} for FKN(l) and FKN(s) at mCX$_3$CR1 (ANOVA; hFKN(s) versus mFKN(l): $p<0.01$; rFKN(s) versus mFKN(l): $p<0.05$).

[d] Comparison of EC_{50} for human, rat and mouse FKN(s) at rCX$_3$CR1 (ANOVA; hFKN(s) versus mFKN(s): $p<0.05$; rFKN(s) versus mFKN(s): $p<0.05$).

[e] Comparison of EC_{50} for human, rat and mouse FKN(s) at mCX$_3$CR1 (ANOVA; hFKN(s) versus rFKN(s): $p<0.01$; rFKN(s) versus mFKN(s): $p<0.001$; mFKN(s) versus hFKN(s): $p<0.001$).

[f] NR: no detectable response.

Viral MIP-2 was able to inhibit rat FKN(s) stimulated [^{35}S]GTPγS binding via both rCX$_3$CR1 and mCX$_3$CR1 (Figure 3). In addition, affinity purified antisera directed against the N-terminal part of the rCX$_3$CR1 was used as a potential

inhibitor of mCX$_3$CR1 mediated [^{35}S]GTPγS binding. Preliminary results revealed a partial block by the anti-CX$_3$CR1 antibodies (Figure 14).

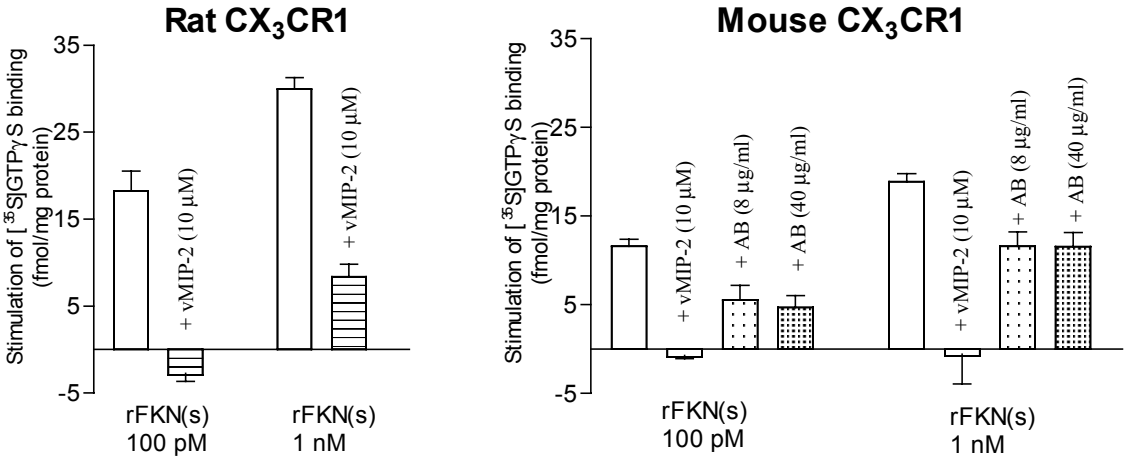

Fig. 14. Inhibition of CX$_3$CR1-mediated [^{35}S]GTPγS-binding stimulated with rat FKN(s). Viral MIP-2 and antisera against the N-terminal domain of rCX$_3$CR1 were used as inhibitors. Stimulation/inhibition was calculated as: [(stimulation – basal [^{35}S]GTPγS-binding)] / [basal [^{35}S]GTPγS-binding]. The results are means of triplicates ± SEM. AB: antibody.

3.4 Intracellular calcium mobilisation

Functional coupling of the rCX$_3$CR1 was further investigated by measuring intracellular calcium mobilisation. Stimulation with human FKN(s) (1µM) was found to elevate intracellular calcium levels shown by an increase in F340/F380 ratio of approximately 0.4 (n=3). A representative experiment is shown in Figure 16. The response was, however, not very robust and not always reproducible.

Viability of the rCX$_3$CR1/HEK-293 cells was confirmed by stimulation with ATP and carbachol, both of which bind to a G-protein coupled receptor. ATP act on P2Y purinergic receptors while carbachol act on muscarinic acethylcholine (mACh) receptors. Figure 15 shows concentration dependent traces for ATP (100 µM – 100 nM) and carbachol (1 mM – 100 nM). In addition, experiments were performed in order to explore whether the P2Y and mACh receptors are rapidly desensitised upon treatment with ATP and

carbachol, respectively. Following the return of intracellular calcium levels back to basal, cells were given an additional dose of substance. It was found that in both cases the response was nearly abolished which may be due to receptor desensitisation (Figure 17).

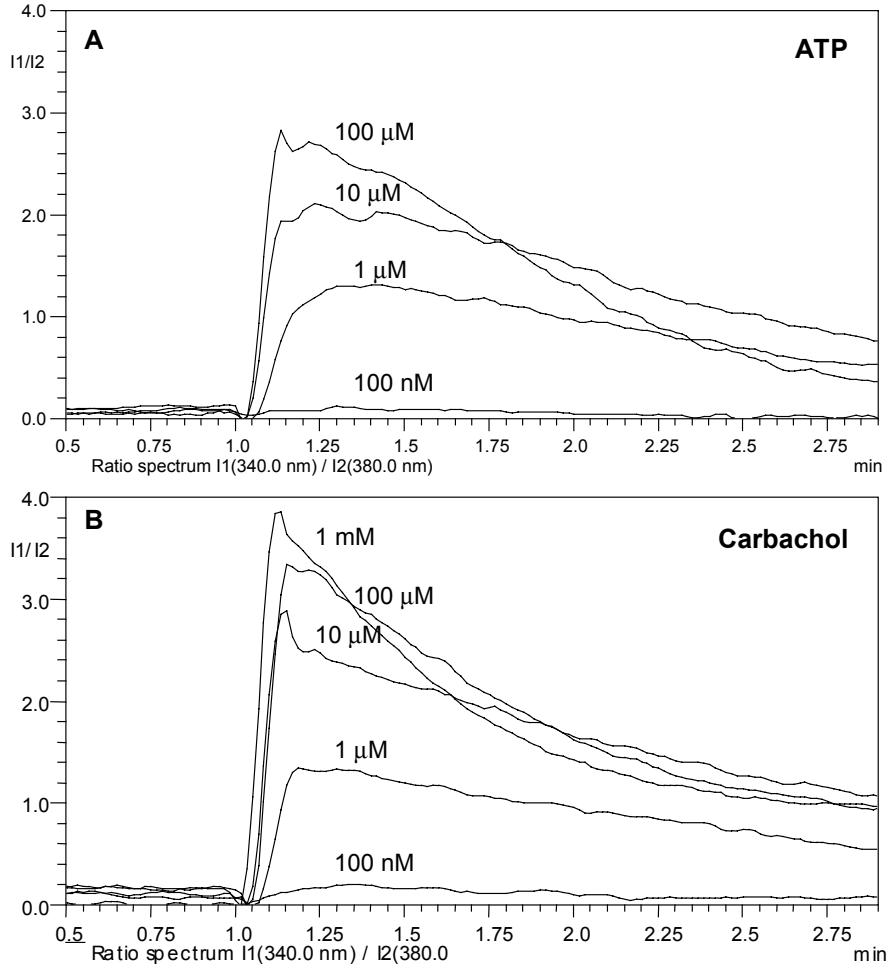

Fig. 15. Concentration dependent intracellular calcium mobilisation in rCX$_3$CR1/HEK-293 cells mediated by ATP (100 µM - 100 nM) (A) and carbachol (1 mM - 100 nM) (B).

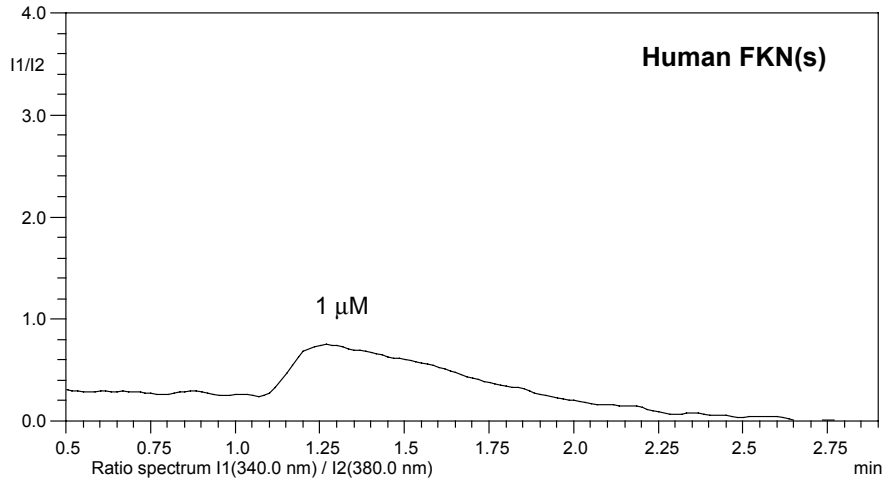

Fig. 16. Intracellular calcium mobilisation induced by human FKN(s) (1μM) in rCX$_3$CR1/HEK-293 cells as measured using Fura-2.

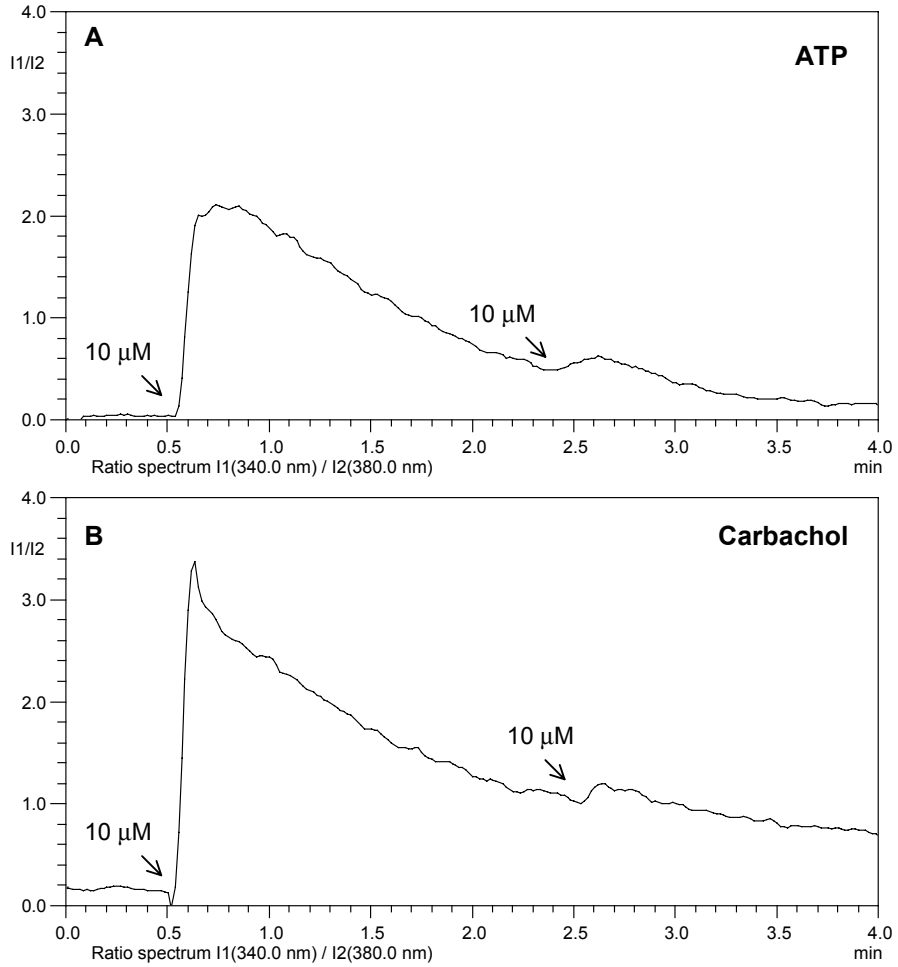

Fig. 17. Intracellular calcium mobilisation in rCX$_3$CR1/HEK-293 cells as measured using Fura-2. Possible desensitisation of P2Y receptors at application of ATP (A) and of mAch receptors at application of carbachol (B). The time of addition is marked with arrows.

4 Discussion

In the present study the *in vitro* pharmacological profiles of human, rat and mouse FKN were investigated. Receptor binding and functional studies were performed at the rat and mouse FKN receptor CX_3CR1 expressed in HEK-293 cells. FKN possesses unique properties compared to other chemokines not only by its cystein motif (CX_3C) but also by being membrane bound. The FKN structure is characterised by a chemokine domain (76 aa) on top of a mucin-like stalk, a transmembrane domain and a short intracellular C-terminal part. The extracellular part (i.e. the chemokine domain and the mucin-like stalk) can be proteolytically cleaved to generate soluble FKN (denoted FKN(l)). This form of FKN is believed to be the soluble form present *in vivo*. The chemokine domain (denoted FKN(s)), thought to be the part that interacts with the receptor, was also investigated in this study.

Saturation binding experiments demonstrated a K_D of 23.6 pM and 30.7 pM for human [^{125}I]FKN(s) binding to the rat and mouse CX_3CR1, respectively. Previous studies presented in the literature have revealed K_D of 100 pM for human FKN(l) to the human CX_3CR1 expressed in K562 cells. Corresponding binding to receptors present on lymphocytes and monocytes revealed K_D of 30 pM and 50 pM, respectively (Imai *et. al.*, 1997).

Competition binding experiments with human, rat and mouse FKN demonstrated an overall tendency of higher affinity for the rCX_3CR1 compared to mCX_3CR1. This was surprisingly true also for mouse FKN, both short and long, that exhibited 4-fold lower affinity for its own receptor compared to the rCX_3CR1.

Significant difference in affinity of FKN(l) compared to FKN(s) was shown at both receptor types with the exception of rat FKN at the rCX_3CR1. Human FKN(s) possessed 10 times higher affinity than human FKN(l) at both rCX_3CR1 and mCX_3CR1. Corresponding comparison for rat was 3-fold. For mouse FKN the opposite relation was true, FKN(l) exhibited an approximate 4-fold higher affinity compared to FKN(s) at both receptors. The soluble form of FKN present *in vivo* is believed to be comprised of the entire extracellular domain i.e. FKN(l) (Bazan *et. al.*, 1997). Interestingly, the isolated chemokine

domain of human and rat FKN i.e. FKN(s) is even more potent at binding than the soluble *in vivo* form.

The rank order of potency for both FKN(l) and FKN(s) were human > rat > mouse at both receptors. The K_i values of human FKN(s) were in good agreement with the K_D values of human [^{125}I]FKN(s) for the same receptor. Mouse FKN(s) possessed very low affinity; 100- and 400-fold lower than human FKN(s) at the rCX_3CR1 and mCX_3CR1, respectively. Corresponding comparison for rat FKN(s) was only 10-fold at both receptors. The deduced amino acid (aa) sequence homology of FKN(s) is; human and rat 83%, human and mouse 78% and rat and mouse 86%. The low affinity of mouse FKN(s) is surprising. It is possible that mouse FKN(s) stabilises a different receptor conformation compared to human and rat FKN(s) but it can not be ruled out that the aa sequence of mouse FKN(s) is wrong (re-sequencing is ongoing by the provider). Exactly what aa are important at receptor binding has not been determined. When comparing human FKN(s) with rat and mouse FKN(s), nine non-conservative aa differences can be observed in both sequences (Figure 11). Three of these differences are the same for both rat and mouse FKN(s). The remaining differences might explain the low affinity of mouse FKN(s) but these differences are also present in mouse FKN(l) and should in that case affect also the binding of the latter. The 5 extra C-terminal aa included in the chemokine domain of mouse FKN (81 aa compared to 76 aa; Pan *et. al.*, 1997; Figure 11) may also affect the affinity of mouse FKN(s). The interaction with the receptor is, however, believed to take place N-terminally at the position of the cystein motif. Exact similarity between FKN(s) and the chemokine domain of FKN(l) has not been confirmed since sequencing of FKN(l) is not performed by the provider.

Competition binding experiments were also performed with the additional forms of rat and mouse FKN(s) (3rFKN(s) and 3mFKN(s)) comprised of three extra aa N-terminally of the chemokine domain. The experiments clearly showed that the three extra aa reduces the affinity of FKN(s) considerably. 3mFKN(s) was the first mouse FKN peptide to appear in the literature (Pan *et. al.*, 1997). It was also the first to be available on the market. Production of mouse FKN(s) without the extra aa was not produced until after the completion of this study (in this study a pre-production sample was used). The

first rat form of FKN(s) on the market was the peptide without the additional aa (Bazan *et. al.*, 1997), whereas 3rFKN(s) was produced later. The three extra aa are here suggested to be part of the signalling peptide that is cleaved off when the protein is expressed on the membrane.

Competition data analysed with one- and two-site curve fitting showed mono-phasic binding in homologous competition (i.e. human [^{125}I]FKN(s) versus human FKN(s)). Competition with rat FKN(s) as well as human and rat FKN(l) were better described with a two-site model. The K_h and K_l values of human, rat and mouse FKN(l) at the rCX_3CR1 were very similar. The proportion of binding to high affinity sites affects, however, the overall K_i. The same data for mCX_3CR1 were not as consistent. When comparing the affinities of the chemokine domain of human, rat and mouse FKN it seems as if human FKN(s) labels exclusively a receptor conformation in a high affinity state or various receptor conformations with the same high affinity. Rat FKN(s) labels both a high- and low affinity conformation and mouse only the low affinity receptor conformation. In the majority of the experiments mouse FKN, both short and long, did not inhibit 100 % of human [^{125}I]FKN(s) binding as defined by 100 nM human FKN(s). This indicates that human FKN(s) labels a receptor conformation not recognised by mouse FKN(s). The GTP-analouge Gpp(NH)p uncouples the receptor causing a shift towards the low affinity state (Figure 3). Studies with rat and mouse FKN(s) in the absence and presence of Gpp(NH)p indicated that G-protein coupling had a slight impact on the conformational state of the receptors, shown by a decrease in agonist affinity in the presence of Gpp(NH)p. This could not be observed for human FKN(s). Saturation binding experiments in the presence of Gpp(NH)p did not show a significant impact on the human [^{125}I]FKN(s) affinity to the rCX_3CR1.

Stimulation of [^{35}S]GTPγS-binding with the various FKN peptides demonstrated a rank order of potency equal to that obtained at competition experiments i.e. human > rat > mouse. Higher potency to the rCX_3CR1 compared to mCX_3CR1 could be observed for human and rat FKN(s) and for human FKN(l). Corresponding comparison for rat and mouse FKN(l) were difficult due to discrepancies between batches/shipments. Later deliveries of mouse FKN(l) exhibited significantly lower potency at both receptor types.

3rFKN(s) and 3mFKN(s) displayed extremely low potency with approximately only half the efficacy of the other FKN peptides.

Experiments with the chemokine receptor antagonist viral MIP-2 displayed very low affinity at the rat and mouse CX_3CR1 (K_i >100 nM). Previous studies have showed considerably higher affinity (EC_{50} = 2 nM) for viral MIP-2 at the rCX_3CR1 (Chen *et. al.*, 1998). Viral MIP-2 had no intrinsic activity but was shown to inhibit CX_3CR1-mediated [^{35}S]GTPγS binding, stimulated with rat FKN(s), at both receptors. Polyclonal CX_3CR1-antibodies directed against the N-terminal part of rCX_3CR1 were able to partially inhibit rat FKN(s) stimulated [^{35}S]GTPγS binding at the mCX_3CR1.

Functional coupling of CX_3CR1 was also explored by measuring intracellular calcium mobilisation. Stimulation of rCX_3CR1/HEK-293 cells with human FKN(s) was performed. Comparison of the various FKN peptides was unfortunately not possible due to a too weak and not always reproducible response. The CX_3CR1 is not normally expressed in HEK-293 cells and the set of G-protein present in the cells may therefore affect the response of second messenger systems associated with the CX_3CR1.

Concluding remarks

Cross-activity studies of human, rat and mouse FKN at the rCX_3CR1 and mCX_3CR1 were performed in this study. Saturation and competition binding experiments were used to profile binding affinites. [^{35}S]GTPγS-binding was used to explore the functional coupling of the receptors. Receptor binding data suggest a higher affinity for rCX_3CR1 compared to mCX_3CR1. The rank order of potency for the various FKN peptides was found to be human > rat > mouse, in both binding and function. Human and rat FKN(s) exhibited higher affinity than the corresponding FKN(l), believed to be present *in vivo*. Mouse FKN(s) exhibited considerably lower affinity compared to the other FKN peptides and it was not able to fully inhibit human [^{125}I]FKN(s) binding. It may be that mouse FKN(s) stabilises a different receptor conformation. Another possible explanation could be inaccuracies in the aa sequence of FKN(s). Further studies are needed in order to fully understand the receptor interaction of these peptides.

5 Acknowledgements

I would like to thank my supervisor Maria Wanderoy for teaching me the laboratory methods I have used in this project. Thanks for supporting me in my writing and for all the laughs during my stay.

I would also like to thank my supervisor Åsa Malmberg for being so positive and patient when helping me to interpret all my data and giving me guidelines for producing this report.

At last I would like to thank all the people at the department of Lead Discovery, AstraZeneca R&D Södertälje, for creating such warm and welcoming atmosphere.

6 References

Asensio VC and Campbell IL (1999) Chemokines in the CNS: plurifunctional mediators in diverse states. *Trends in Neurosciences* 22: 504-512

Bazan JF, Bacon KB, Hardiman G, Wang W, Soo K, Rossi D, Greaves DR, Zlotnik A and Schall TJ (1997) A new class of membrane-bound chemokine with a CX_3C motif. *Nature* 385: 640-644

Bosworth N and Towers P (1989) Scintillation proximity assay. *Nature* 341: 167-168

Chen S, Bacon BK, Li L, Garcia GE, Xia Y, Lo D, Thompson DA, Siani MA, Yamamoto T, Harrison JK and Feng L (1998) In Vivo Inhibition of CC and CX_3C Chemokine-induced Leukocyte Infiltration and Attenuation of Glomerulonephritis in Wistar-Kyoto (WKY) Rats by vMIP-II *J Exp Med* 188: 193-198

Cheng Y-C and Prusoff WH (1973) Relationship Between the Inhibition Constant (K_I) and the Concentration Inhibitor which Causes 50 Percent Inhibition (I_{50}) of an Enzymatic Reaction. *Biochem Pharmacol* 22: 3099-3108

Chapman GA, Moores K, Harrison D, Campbell CA, Stewart BR and Strijbos PJLM (2000) Fractalkine Cleavage from Neuronal Membranes Represent an Acute Event in the Inflammatory Response to Excitotoxic Brain Damage. *J Neuroscience* 20: 1-5

Fong AM, Erickson HP, Zachariah JP, Poon S, Schamberg NJ, Imai T and Patel DD (2000) Ultrastructure and Function of the Fractalkine Mucin Domain in CX_3C Chemokine Domain Presentation. *J Biol Chem* 275: 3781-3786

Grynkiewicz G, Poenie M and Tsien RY (1985) A New Generation of Ca2+ Indicators with Greatly Improved Fluorescence Properties. *J Biol Chem* 260: 3440-3450

Harrington CR (1990) Lowry Protein Assay Containing Sodium Dodecyl Sulfate in Microtiter Plates for Protein Determinations on Fractions from Brain Tissue. *Anal Biochem* 186: 285-287

Harrison JK, Jiang Y, Chen S, Xia Y, Maciejewski D, McNamara RK, Streit WJ, Salafranca MN, Adhikari S, Thompson DA, Botti P, Bacon KB and Feng L (1998) Role of neuronally derived fractalkine in mediating interactions between neurons and CX3CR1-expressing microglia. *Proc Natl Acad Sci USA* 95: 10896-10901

Imai T, Hieshima K, Haskell C, Baba M, Nagira M, Nishimura M, Kakizaki M, Takagi S, Nomiyama H, Schall TJ and Yoshie O (1997) Identification and Molecular Characterization of Fractalkine Receptor CX_3CR1, which Mediates Both Leukocyte Migration and Adhesion. *Cell* 91: 521-530

Kent RS, De Lean A and Lefkowitz R (1980) A Quantitative Analysis of Beta-Adrenergic Receptor Interactions: Resolution of High and Low Affinity States of the Receptor by Computer Modeling of Ligand Data. *Mol Pharmacol* 17: 14-23

Lorenzen A, Fuss M, Vogt H and Schwabe U (1993) Measurement of Guanine Nucleotide-Binding Protein Activation by A_1 Adenosine Receptor Agonists in Bovine Brain Membranes: Stimulation of Guanosine-5'-O-(3-[^{35}S]thio)triphosphate Binding. *Mol Pharmacol* 44: 115-123

Lowry OJ, Rosebrough NJ, Farr AL and Randall RJ (1951) Protein Measurement with the Folin Phenol Reagent. *J Biol Chem* 193: 256-275

Luster AD (1998) CHEMOKINES – CHEMOTACTIC CYTOKINES THAT MEDIATE INFLAMMATION. *New England Journal of Medicine* 338: 436-445

Milligan G and Unson CG (1989) Persistent activation of the alpha subunit of Gs promotes its removal from the plasma membrane. *Biochem J* 260: 837-841

Morris AJ and Scarlata S (1997) Regulation of Effectors by G-protein α- and $\beta\gamma$-Subunits. *Biochem Pharmacol* 54: 429-435

Noseworthy JH (1999) Progress in determining the causes and treatment of multiple sclerosis. *Nature* 399: A 40-A 46

Pan Y, Lloyd C, Zhou H, Dolich S, Deeds J, Gonzalo J-A, Vath J, Gosselin M, Ma J, Dussault B, Woolf E, Alperin G, Culpepper J, Gutierrez-Ramos JC and Gearing D (1997) Neurotactin, a membrane-anchored chemokine upregulated in brain inflammation. *Nature* 387: 611-617

Raport CJ, Schweickart VL, Eddy Jr RL, Shows TB and Gray PW (1995) The orphan G-protein-coupled receptor-encoding gene V28 is closely related to genes for chemokine receptors and is expressed in lymphoid and neural tissues. *Gene* 163: 295-299

Udenfriend S, Gerber L and Nelson N (1987) Scintillation Proximity Assay: A Sensitive Continuous Isotopic Method for Monitoring Ligand/Receptor and Antigen/Antibody Interactions. *Analytical Biochemistry* 161: 494-500

van Acker FAA, Voss H-P and Timmerman H (1996) Chemokines – structure, receptors and functions . A new target for inflammation and asthma therapy? *Mediators of Inflammation* 5: 393-416

Wieland T and Jacobs KH (1994) Measurement of Receptor-Stimulated Guanosine 5'-O-(γ-Thio)triphosphate Binding by G Proteins. *Methods in Enzymology* 237: 3-13